

# MLorc: Momentum Low-rank Compression for Large Language Model Adaptation

Wei Shen<sup>1\*</sup>, Zhang Yaxiang<sup>2\*†</sup>, Minhui Huang<sup>3</sup>, Mengfan Xu<sup>4</sup>, Jiawei Zhang<sup>5</sup>, Cong Shen<sup>1</sup>

<sup>1</sup> University of Virginia, <sup>2</sup> National University of Singapore, <sup>3</sup> Meta

<sup>4</sup> University of Massachusetts at Amherst, <sup>5</sup> University of Wisconsin-Madison

## Abstract

With the increasing size of large language models (LLMs), full-parameter fine-tuning imposes substantial memory demands. To alleviate this, we propose a novel memory-efficient training paradigm called **Momentum Low-rank compression (MLorc)**. By directly compressing and reconstructing momentum rather than gradients, MLorc avoids imposing a fixed-rank constraint on weight update matrices and better preserves the training dynamics of full-parameter fine-tuning, in contrast to existing low-rank approaches such as LoRA and GaLore. Empirically, MLorc consistently outperforms other memory-efficient training methods, matches or even exceeds the performance of full fine-tuning with a small rank (e.g.,  $r = 4$ ), and generalizes well across different optimizers – all while not compromising time or memory efficiency. Furthermore, we provide a theoretical guarantee for its convergence under reasonable assumptions.

## 1 Introduction

Large Language Models (LLMs) have demonstrated strong generalization capabilities on downstream tasks after fine-tuning [Liu et al., 2019, Raffel et al., 2020, Li and Liang, 2021]. However, full-parameter fine-tuning is prohibitively expensive in terms of GPU memory. In addition to storing billions of model parameters and activation values, training also requires memory for gradients and various optimizer states (e.g., first- and second-order momentum terms in Adam). Without memory-saving techniques, standard AdamW consumes approximately three times more memory for gradients and optimizer states than for storing model parameters alone.

One promising approach to reduce this memory overhead is to design memory-efficient optimization paradigms tailored for fine-tuning, where the objective is to adapt the model to specific tasks. LoRA (Low-Rank Adaptation) [Hu et al., 2022] is one of the most widely adopted parameter-efficient fine-tuning (PEFT) methods: it freezes the original model weights and introduces trainable, low-rank updates. However, LoRA inherently limits the space of possible weight updates due to its low-rank constraint, and its reparameterization can significantly alter training dynamics. Prior studies have shown that LoRA may underperform full-parameter fine-tuning on certain tasks [Biderman et al., 2024, Xia et al., 2024] and exhibit distinct update patterns [Liu et al., 2024b].

Recently, GaLore [Zhao et al., 2024], another memory-efficient optimization approach, has garnered attention. GaLore projects gradients and optimizer states (e.g., momentum) into a low-dimensional subspace for storage and uses the same projector to reconstruct optimizer states used to update weight. The projectors are periodically updated through Singular Value Decomposition (SVD) on stochastic gradient matrices. GaLore claims to overcome the limitations of low-rank methods like LoRA by canceling low-rank factorization and improving training dynamics. Nevertheless, both prior research [Luo et al., 2024] and our experiments reveal that GaLore usually underperforms, even compared to LoRA. We attribute this to suboptimal training dynamics, that is, the reconstruction in GaLore can break the structure of the momentum, due to the instability of singular vectors of the stochastic gradient. We will analyze this in detail in Section 3.

\*Equal contribution. The first two authors are listed in alphabetical order.

†Corresponding author: Zhang Yaxiang, e1353410@u.nus.edu.

To address these challenges, we propose a new memory-efficient training paradigm, **Momentum Low-rank compression (MLorc)**. Unlike existing low-rank approaches such as LoRA and GaLore, MLorc directly compresses and reconstructs momentum instead of gradients with Randomized SVD (RSVD) [Halko et al., 2011] and then uses these compressed momentum to run some benchmark optimizers like Adam or Lion, thereby avoiding fixed-rank constraints on weight updates and maintaining closer alignment with the training dynamics of full-parameter fine-tuning. The motivation of designing this algorithm is that we empirically verify the approximated low-rank structure of momentum throughout training and so compressing the momentum will not lose too much information. Moreover, directly compressing the momentum can avoid the affect of unstable stochastic gradient.

We validate the effectiveness of MLorc through extensive experiments across various models, datasets, and optimizers. MLorc outperforms LoRA [Hu et al., 2022] and GaLore [Zhao et al., 2024] on math and coding tasks. Meanwhile, it maintains competitive time and memory efficiency relative to other memory-saving methods. On LLaMA2-7B, MLorc achieves comparable training time and memory usage to LoRA. Additionally, we provide a theoretical convergence guarantee for MLorc with the Lion optimizer, matching the original Lion’s convergence rate under reasonable assumptions Dong et al. [2024].

The remainder of this paper is organized as follows. Section 2 reviews related work. Section 3 critically examines the limitations of current memory-efficient training paradigms, and then introduces our novel methodology, followed by detailed memory and convergence analyses. Section 4 presents the experimental results. Finally, Section 5 concludes the paper and outlines potential directions for future research.

## 2 Related Works

**Low-rank adaptation.** Low-rank adaptation methods, such as LoRA [Hu et al., 2022], have been proposed to enhance the memory efficiency of fine-tuning large language models. LoRA introduces trainable low-rank matrices into each layer of a pre-trained model, significantly reducing the number of trainable parameters while maintaining performance comparable to full fine-tuning. Inspired by LoRA, Flora [Hao et al., 2024] periodically resamples random projection matrices during training to compress the gradients, aiming to achieve higher-rank updates over time while maintaining same level memory consumption. There are also other variants of LoRA designed for improving performance and other purposes [Meng et al., 2024, Kalajdziewski, 2023, Dettmers et al., 2023, Hayou et al., 2024, Zhang et al., 2023b, Li et al., 2024, Zi et al., 2023, Wang et al., 2023b, Li et al., 2024, Zhang et al., 2023a]. In contrast, GaLore (Gradient Low-Rank Projection) [Zhao et al., 2024] is a memory-efficient fine-tuning method that reduces the storage cost of gradients and optimizer states by projecting them into a dynamically learned low-rank subspace. Unlike LoRA, which applies low-rank adaptations directly to weight updates, GaLore maintains full-parameter training while compressing optimizer states, but its reliance on periodic SVD introduces additional computational overhead. There are also other variants of GaLore designed for improving time efficiency and further reducing memory footprint. Beyond the original version, subsequent variants of GaLore have been developed to enhance time efficiency and further minimize memory footprint [Zhang et al., 2024, Rajabi et al., 2025, Yang et al., 2025]. In contrast, our MLorc method achieves closer alignment with full-parameter fine-tuning by intelligently handling momentum.

**Memory-efficient optimization.** There are also other techniques to reduce memory footprint during training, including gradient checkpointing [Chen et al., 2016], quantization [Dettmers et al., 2022, Li et al., 2023] and other memory-efficient optimization methods (AdaLomo [Lv et al., 2023], MeZO [Malladi et al., 2023], etc). These methods address different aspects of the memory bottleneck. They are orthogonal to our methods and some of them can be combined with MLorc to further reduce the memory footprint.

**Matrix compression.** Matrix compression techniques, particularly those based on Singular Value Decomposition (SVD), play an important role in model compression [Wang et al., 2025, Liu et al., 2024a] and reducing memory footprint [Zhao et al., 2024] in model training. Randomized SVD (RSVD) [Halko et al., 2011] is an efficient variant of SVD. SVD decomposes a matrix into low-rank components that preserve most of its information, while RSVD accelerates this process by approximating the dominant singular subspace using random projections. These methods enable compact representation of gradients and optimizer states, thus laying the foundation of our method.

### 3 Our method

In this section, we introduce our main method. We begin by presenting the preliminaries on which our method is built, including LoRA and GaLore. We then formally elaborate on MLorc, covering the algorithmic framework and steps, memory analysis, and convergence analysis.

#### 3.1 Preliminaries

##### 3.1.1 LoRA

Low-Rank Adaptation (LoRA) [Hu et al., 2022] is a parameter-efficient fine-tuning technique designed for adapting large pre-trained models to downstream tasks. Instead of updating the full model weights, LoRA freezes the original parameters and injects trainable low-rank matrices into specific layers (typically attention or feedforward layers). This significantly reduces the number of trainable parameters and memory requirements during fine-tuning. Initial weight of the model  $W_0 \in R^{m \times n}$  is frozen, and weight update is achieved by updating two low rank matrices:  $B \in R^{m \times r}$  and  $A \in R^{r \times n}$ , typically  $r \ll m, n$ , as illustrated in the following formula:

$$W = W_0 + BA. \quad (1)$$

Despite its memory efficiency, LoRA has several limitations. First, the imposed low-rank constraint can restrict the expressiveness of weight updates, potentially limiting performance on tasks that require more complex adaptations. Second, LoRA introduces a reparameterization of the weight update process, which alters the training dynamics and can lead to suboptimal convergence in some scenarios [Zhao et al., 2024, Meng et al., 2024]. Empirical studies have shown that LoRA can underperform full fine-tuning on certain tasks [Biderman et al., 2024, Xia et al., 2024].

##### 3.1.2 GaLore

GaLore (Gradient Low-Rank Projection) [Zhao et al., 2024] is a recent memory-efficient training paradigm designed to reduce the memory footprint of optimizer states and gradients during fine-tuning of large language models. Unlike LoRA, which freezes the model and injects low-rank trainable adapters into the weight matrices, GaLore applies a low-rank projection directly to the gradients and optimizer states. Specifically, it performs periodic Singular Value Decomposition (SVD) on the gradients to identify a low-rank subspace, into which the optimizer states (e.g., momentum, variance) are projected. This strategy allows GaLore to maintain full-parameter weight updates while significantly compressing the memory required for training, aiming to preserve training dynamics more faithfully than LoRA’s reparameterized updates.

However, there is still room for improvement in GaLore. Although GaLore does not constrain the weight updates themselves to be low-rank, it relies on fixed (over a certain number of steps) low-rank projections, which may still limit its ability to fully capture dynamic gradient information.

To be specific, in step  $t$ , GaLore (on Adam) first gets projector  $P_t$ : it is updated every  $T$  steps using the singular vector of gradient  $G_t$ ; otherwise  $P_t$  is equal to  $P_{t-1}$ . Subsequently, GaLore projects  $G_t$ :  $R_t = P_t^T G_t$  and first/second order momentum  $M_t, V_t$  is constructed by exponential average of  $R_t$ , just like original Adam. Finally, low-rank update  $N_t = \frac{M_t}{\sqrt{V_t + \epsilon}}$  and GaLore uses  $P_t$  to project back  $N_t$ . To ensure GaLore’s training dynamics align with those of full-parameter training, it implicitly depends on two key assumptions: (1) gradients exhibit a low-rank structure, and (2) gradients change slowly across training steps. While the first assumption is well-supported by prior studies [Zhao et al., 2022, Cosson et al., 2023], the second is questionable in the context of mini-batch training. Infrequent projector updates can result in misaligned projections and reconstructions, and even with expensive high-frequency updates, a critical limitation remains: **there exists no well-defined projector for back-projection of  $N_t$** , since momentum is an accumulation (i.e., weighted average) of mini-batch gradients across different steps. For example, with default  $\beta_2 = 0.999$ , gradients of 100 steps earlier still have comparable weight with current gradients in second-order momentum; hence,  $M_t$  and  $V_t$ ’s eigen space is very different from  $g_{t-\tau}$ ’s for any  $\tau$ , not to mention  $N_t$  is a non-linear transformation of  $M_t$  and  $V_t$ . Consequently,  $N_t$ ’s eigenspace cannot be recovered from any single-step gradient’s eigenspace. In fact, GaLore [Zhao et al., 2024] does not have a theoretical proof involving momentum: it only analyzes GaLore with gradient descent. This motivates us to shift focus from gradient compression to

momentum compression – **directly compressing and reconstructing momentum rather than gradients**.

### 3.2 MLorc

For a matrix  $A \in \mathbb{R}^{m \times n}$ , we denote its Frobenius norm as  $\|A\|_F$ , denote its entrywise  $l_1$  norm as  $\|A\|_{1,1} \triangleq \sum_{i=1}^m \sum_{j=1}^n |A_{ij}|$ . Given a batch sample  $B = \{\xi^i\}_{i=1}^b$ , we denote  $\nabla f(W; B) = \frac{1}{b} \sum_{i=1}^b \nabla f(W; \xi_i)$ .

#### 3.2.1 Algorithm and Implementation

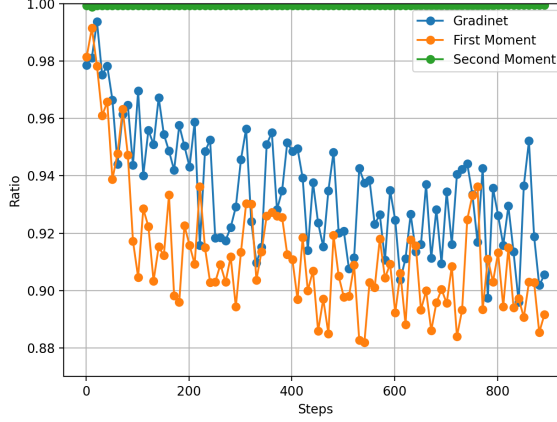


Figure 1: Ratio of top-8 singular values to total singular values for gradient, first moment, and second moment during AdamW finetuning of RoBERTa-base on the STSB dataset.

To enable compression at the momentum level, we first investigate whether momentum exhibit low-rank structure. We analyze various components involved in optimization by examining the concentration of singular values in gradients and momenta. As illustrated in Figure 1, the first-order momentum shows a spectral pattern similar to that of the gradients, while the second-order momentum demonstrates an even stronger low-rank structure. More experimental evidence can be found in Appendix C.1. Motivated by these empirical observations, along with our earlier analysis of GaLore’s training dynamics, we propose **Momentum Low-rank compression (MLorc)**, a new memory-efficient training paradigm for large-scale model fine-tuning.

The core idea of MLorc is to efficiently and accurately compress momentum for storage and reconstruct momentum to update weight, and we chose RSVD [Halko et al., 2011] to do this. A detailed introduction to RSVD is deferred to Appendix A. Here, we highlight a key property: the time complexity of RSVD is  $O(mnr)$ , which is on the same order as the projection and back-projection operations. Notably, MLorc can be applied to any optimizer (e.g, Adam, Lion) with momentum. Taking AdamW as an example: at each optimization step, we first reconstruct the first and second order momentum  $\tilde{m}_{t-1}, \tilde{v}_{t-1}$  from the compressed optimizer state:  $\tilde{m}_{t-1} = m_{u,t-1}m_{s,t-1}m_{v,t-1}^\top$ ,  $\tilde{v}_{t-1} = v_{u,t-1}v_{s,t-1}v_{v,t-1}^\top$ , update them using the current gradient:  $m_t = \beta_1\tilde{m}_{t-1} + (1 - \beta_1)g_t$ ,  $v_t = \beta_2\tilde{v}_{t-1} + (1 - \beta_2)g_t^2$ , and then compress the updated momenta using RSVD:  $(m_{u,t}, m_{s,t}, m_{v,t}) = \text{RSVD}(m_t)$ ,  $(v_{u,t}, v_{s,t}, v_{v,t}) = \text{RSVD}(v_t)$ . Finally, we use these updated momenta to perform the usual parameter update.

There is also a special consideration for second-order momentum, which must remain entry-wise non-negative. A straightforward approach is to apply an entry-wise *ReLU* to the reconstructed second-order momentum  $\tilde{v}_{t-1}$ . However, this introduces zeros in the reconstructed values, and since  $\beta_2$  is typically set very close to 1, these zeros can result in extremely small values in the updated second-order momentum. This can destabilize training and degrade model performance. To address this, we add a small constant entry-wise to the zero values introduced by *ReLU*. Given that parameter groups often have different scales, this constant should be chosen adaptively. In practice, we set it to the absolute mean of the negative part of the reconstructed momentum, i.e,  $\text{abs}(\text{mean}(\tilde{v}_{t-1} - \text{ReLU}(\tilde{v}_{t-1})))$  (which is usually much smaller than the positive part). This modification is different from adding  $\epsilon$

on the square root of second-order momentum: 0s here come from the error introduced by momentum compression rather than the small magnitude of the corresponding gradient element.

---

**Algorithm 1** MLorc-AdamW

---

```

1: Input: Initial weights  $W_0$ , learning rate  $\alpha$ , betas  $\beta_1, \beta_2$ , weight decay rate  $\lambda$ , constant  $\varepsilon$ , target rank  $r$ , oversampling parameter  $p$ , batch size  $b$ .
2: Initialize RSVD factors:  $(m_{u,0}, m_{s,0}, m_{v,0}) \leftarrow 0, (v_{u,0}, v_{s,0}, v_{v,0}) \leftarrow 0, t \leftarrow 0$ 
3: while not converged do
4:    $t \leftarrow t + 1$ 
5:   Sample a mini-batch  $B_t = \{\xi_t^i\}_{i=1}^b$  uniformly at random
6:   Compute gradient:  $g_t \leftarrow \nabla f(W_{t-1}; B_t)$ 
7:    $\tilde{m}_{t-1} \leftarrow m_{u,t-1} m_{s,t-1} m_{v,t-1}^\top$ 
8:    $\tilde{v}_{t-1} \leftarrow v_{u,t-1} v_{s,t-1} v_{v,t-1}^\top$ 
9:    $\tilde{v}_{t-1} \leftarrow \text{ReLU}(\tilde{v}_{t-1}) + \text{abs}(\text{mean}(\tilde{v}_{t-1} - \text{ReLU}(\tilde{v}_{t-1})))$ 
10:  # Do note that mean here only averages over non-zero elements(negative parts), and zero elements remain unchanged.
11:   $m_t \leftarrow \beta_1 \tilde{m}_{t-1} + (1 - \beta_1) g_t$ 
12:   $v_t \leftarrow \beta_2 \tilde{v}_{t-1} + (1 - \beta_2) g_t^2$ 
13:   $(m_{u,t}, m_{s,t}, m_{v,t}) \leftarrow \text{RSVD}(m_t, r, p)$ 
14:   $(v_{u,t}, v_{s,t}, v_{v,t}) \leftarrow \text{RSVD}(v_t, r, p)$ 
15:   $\hat{m}_t \leftarrow \frac{m_t}{1 - \beta_1^t}$ 
16:   $\hat{v}_t \leftarrow \frac{v_t}{1 - \beta_2^t}$ 
17:   $W_t \leftarrow W_{t-1} - \alpha(\frac{\hat{m}_t}{\sqrt{\hat{v}_t + \varepsilon}} + \lambda W_{t-1})$ 
18: end while
19: return  $W_t$ 

```

---

Algorithm 1 shows the detailed description of MLorc-AdamW. Do note that *mean* here only averages over non-zero elements(negative parts), and zero elements remain unchanged. Similarly, the high-level idea of MLorc can also be applied to other optimizers, such as Lion [Chen et al., 2023]. The following Algorithm 2 shows a detailed description of MLorc-Lion.

---

**Algorithm 2** MLorc-Lion

---

```

Input: Initial weights  $W_0$ , learning rate  $\alpha$ , betas  $\beta_1, \beta_2$ , target rank  $r$ , oversampling parameter  $p$ , batch size  $b$ .
2: Initialize RSVD factors:  $(m_{u,0}, m_{s,0}, m_{v,0}) \leftarrow 0, t \leftarrow 0$ 
   while not converged do
4:    $t \leftarrow t + 1$ 
   Sample a mini-batch  $B_t = \{\xi_t^i\}_{i=1}^b$  uniformly at random
6:   Compute gradient:  $g_t \leftarrow \nabla f(W_{t-1}; B_t)$ 
    $\tilde{m}_{t-1} \leftarrow m_{u,t-1} m_{s,t-1} m_{v,t-1}^\top$ 
8:    $c_t \leftarrow \beta_1 \cdot \tilde{m}_{t-1} + (1 - \beta_1) \cdot g_t$ 
    $m_t \leftarrow \beta_2 \cdot \tilde{m}_{t-1} + (1 - \beta_2) \cdot g_t$ 
10:   $(m_{u,t}, m_{s,t}, m_{v,t}) \leftarrow \text{RSVD}(m_t, r, p)$ 
    $W_t \leftarrow W_{t-1} - \alpha \cdot \text{sign}(c_t)$ 
12: end while
   return  $W_t$ 

```

---

### 3.2.2 Memory Consumption Analysis

GPU memory consumption during large language model (LLM) training primarily comes from four sources: model weights, gradients, optimizer states, and activation values. Among these, weight and activation memory usage is independent of the optimizer choice. Therefore, we focus our analysis on the remaining two components: gradients and optimizer states.

In fine-tuning scenarios, the rank  $r$  used in low-rank memory-efficient training methods including LoRA [Hu et al., 2022], GaLore [Zhao et al., 2024] and our method, is typically much smaller than

the dimensionality of the weight matrices (e.g,  $r = 4$  or  $r = 8$ ) [Hu et al., 2022, Zhao et al., 2024]. As a result, the memory overhead associated with optimizer states becomes negligible. The situation is more nuanced for gradients. Methods like LoRA and its variants naturally reduce gradient memory usage, since they only require storing gradients with respect to a small number of low-rank trainable parameters. In contrast, approaches like our MLorc and GaLore may avoid storing full gradients by performing per-layer weight updates. It is also worth noting that gradients do not always contribute to peak memory usage: for reasonably large batch sizes (in our experiments, 32 for LLaMA2-7B [Touvron et al., 2023], even with gradient checkpointing), the peak memory footprint often occurs during the forward pass, when all activation values must be stored.

Taken together, these observations suggest that MLorc can indeed achieve memory efficiency comparable to that of LoRA – a claim that is further supported by our empirical results in Section 4 and Appendix C.2.

### 3.2.3 Convergence analysis

In this section, we present a convergence analysis of MLorc-Lion (Algorithm 2), demonstrating that it can achieve the same convergence rate as the original Lion optimizer [Chen et al. [2023], Dong et al. [2024]]. Lion is a well-known optimizer and often achieves performance comparable to AdamW when optimizing neural networks. Lion utilizes the sign function to adjust the update magnitude of each component, which is conceptually similar to AdamW. In this work, we demonstrate the theoretical guarantees of our MLorc framework by presenting the convergence analysis of MLorc-Lion. The extension to MLorc-AdamW is left for future work. We consider optimizing loss function  $f : \mathbb{R}^{m \times n} \rightarrow \mathbb{R}$ . And we use the following standard assumptions. These assumptions also appear in the analysis of original optimizers [Arjevani et al., 2023, Wang et al., 2023a, Reddi et al., 2019].

**Assumption 3.1.** The loss function  $f$  is  $L$ -Lipschitz smooth, i.e. for any  $W, W' \in \mathbb{R}^{m \times n}$ , we have

$$\|\nabla f(W) - \nabla f(W')\|_F \leq L\|W - W'\|_F.$$

**Assumption 3.2.**  $\nabla f(W; \xi)$  is an unbiased stochastic estimator of the true gradient  $\nabla f(W)$  and have a bounded variance, i.e.

$$\begin{aligned} \mathbb{E}[\nabla f(W; \xi)] &= \nabla f(W) \\ \mathbb{E}\|\nabla f(W; \xi) - \nabla f(W)\|_F^2 &\leq \sigma^2. \end{aligned}$$

We mention that momentum is observed to be of nearly low-rank. Hence, we make the following approximate low-rank assumption, which controls the ratio of tail singular values of momentum in MLorc-Lion.

**Assumption 3.3.** For any  $m_t$ ,  $t = 0, 1, 2, \dots$ , generated by Algorithm 2 and  $\sigma_1^t \geq \sigma_2^t \geq \dots$  are  $m_t$ 's singular values, we assume

$$\left( \sum_{j>r} (\sigma_j^t)^2 \right)^{\frac{1}{2}} \leq \rho \|m_t\|_F, \text{ for } t = 0, 1, 2, \dots$$

With these assumptions, we have following theorem.

**Theorem 3.4** (informal). *When Assumptions 3.1, 3.2 and 3.3 hold, applying Algorithm 2 with appropriate parameters and assuming  $\rho = O((1 - \beta_2)d^{-1/2})$ , then we can find  $t = O(Ld^2\sigma^2\epsilon^{-4})$  such that  $\mathbb{E}[\|\nabla f(W_t)\|_{1,1}] \leq O(\epsilon)$ , where  $d = mn$ , matching the same convergence rate as the original Lion.*

The formal statement and proofs of Theorem 3.4 can be found in Appendix B.

## 4 Experiments

### 4.1 Experiments on NLG tasks with LLaMA2-7B

In this section, we evaluate MLorc's performance on large language models, focusing on NLG (Natural Language Generation) tasks. We fine-tuned LLaMA 2-7B [Touvron et al., 2023] on two tasks: math



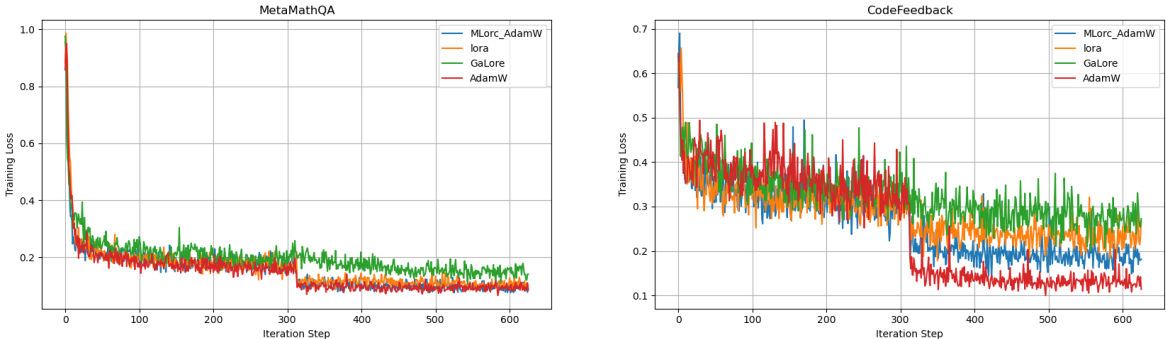
and code. To demonstrate the effectiveness of MLorc, We compare MLorc’s performance on AdamW with Full AdamW, LoRA [Hu et al., 2022], and GaLore [Zhao et al., 2024] (both optimized by AdamW). We also compare MLorc’s performance on MLorc-Lion [Chen et al., 2023] with Full Lion to explore its applicability to different optimizers. Experimental results suggest that MLorc significantly reduces training loss during optimization and improves validation accuracy on test datasets.

**Experimental Setup.** For the math task, the model was fine-tuned LLaMA 2-7B on the MetaMathQA dataset [Yu et al., 2023] and evaluated on GSM8K [Cobbe et al., 2021] validation sets. For the code task, the model was fine-tuned on the CodeFeedback dataset [Zheng et al., 2024] and evaluated on the HumanEval [Chen et al., 2021] dataset. All experiments were conducted on 1 H100-96 GPU, using subsets of training datasets containing 10K data points and were trained for 2 epochs. We use a rank=4 for all memory-efficient training paradigm, a batch size of 32 with gradient checkpointing and without gradient accumulation, a linear learning rate scheduler with a warmup ratio of 0.03. We set learning rate after tuning on each method and each dataset. It is worth mentioning that we set  $\beta_1$  of MLorc-AdamW as 0.8 rather than the default value 0.9, in order to mitigate the influence of approximation error arising from RSVD. More hyperparameter setups, such as specific learning rates and oversampling parameters, can be found in Appendix D.1. Average accuracy over four evaluations and the standard deviation of accuracy is reported in Table 1.

Table 1: Results of LLaMA 2-7B fine-tuned on math and code tasks. MLorc consistently outperforms other memory-efficient training paradigms.

Method(r=4)	GSM8K	HumanEval
Full(AdamW)	47.69 $\pm$ 0.15	21.96 $\pm$ 0.46
MLorc(AdamW)	47.37 $\pm$ 1.09	20.70 $\pm$ 0.42
LoRA	46.20 $\pm$ 0.46	18.45 $\pm$ 1.07
GaLore	38.89 $\pm$ 0.73	17.25 $\pm$ 0.49
Full(Lion)	46.38 $\pm$ 1.11	18.00 $\pm$ 0.30
MLorc(Lion)	47.75 $\pm$ 0.25	18.75 $\pm$ 0.78

As shown in Table 1, MLorc outperforms LoRA [Hu et al., 2022] and GaLore [Zhao et al., 2024] on both math and coding task, significantly reduces accuracy gap between Full-parameter fine-tuning and existing memory-efficient training paradigms, demonstrating its ability in handling complex tasks on large language models. Additionally, the optimal learning rate of MLorc is much closer to Full-parameter fine-tuning than LoRA or GaLore (see Appendix D), which suggests it might have similar training dynamics and indicates its utility in accelerating convergence.

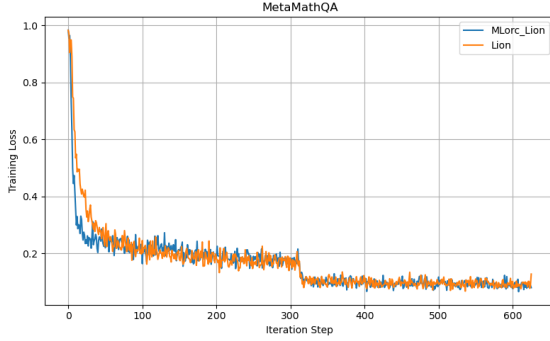


(a) Training Loss on MetaMathQA[Yu et al., 2023] dataset

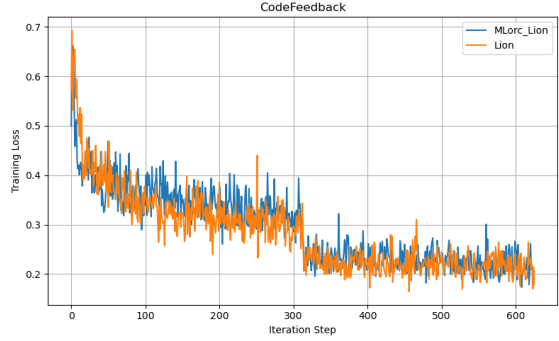
(b) Training Loss on CodeFeedback[Zheng et al., 2024] dataset

Figure 2: Training Loss of AdamW of different methods

**Training Loss Curve.** As shown in Figure 2 and 3, the training loss of MLorc is consistently smaller than LoRA [Hu et al., 2022] and GaLore [Zhao et al., 2024], and is usually close to the full version, whenever in AdamW or Lion. This shows that MLorc behaves similarly to the full version,



(a) Training Loss on MetaMathQA[Yu et al., 2023] dataset



(b) Training Loss on CodeFeedback[Zheng et al., 2024] dataset

Figure 3: Training Loss of Full Lion and Lion with MLorc

hence providing strong evidence for its effectiveness.

Table 2: Memory consumption of different methods with AdamW optimizer when training on MetaMathQA[Yu et al., 2023]. Hyperparameters and other settings are same as previous experiments.

Full-FT	MLorc	GaLore	LoRA(default)	LoRA(Full)
66.5GB	39.3GB	39.3GB	36.5GB	40.1GB

**Time and Memory Efficiency.** Table 2 compares memory consumption between different training methods. Memory consumption of MLorc and GaLore is almost the same; there is a difference between MLorc and LoRA (in default setting), and we attribute this to the different parameter group they optimize over: LoRA does not tune the embedding layer. When we use LoRA with the same parameter group as MLorc, it is in fact less memory-efficient than MLorc.

Table 3: Training time of different memory-efficient training methods with AdamW optimizer when training on MetaMathQA [Yu et al., 2023]. Hyperparameters and other settings are the same as the previous experiments.

MLorc	LoRA(default)	GaLore
1h2min	1h3min	1h8min

Table 3 compares training time between different memory-efficient training methods. Experimental result shows that MLorc achieves time efficiency comparable to that of LoRA [Hu et al., 2022] and reduces training time compared to GaLore [Zhao et al., 2024], confirming that the additional overhead from compression and reconstruction is negligible in practical fine-tuning scenarios.

## 4.2 Experiments on Natural Language Understanding Tasks

In this section, we assess the effectiveness of MLorc in fine-tuning language models for natural language understanding (NLU) tasks. Specifically, we fine-tune pre-trained RoBERTa models [Liu et al., 2019] on the GLUE benchmark [Wang et al., 2018] using MLorc-AdamW, and compare its performance against full fine-tuning, LoRA [Hu et al., 2022], and GaLore [Zhao et al., 2024]. As shown in Table 4, MLorc significantly outperforms GaLore, surpasses LoRA on most tasks, and achieves overall performance comparable to that of full fine-tuning. Detailed experimental settings can be found in Appendix D.2.

We also performed experiments to examine the low-rank structure of the gradient, first-order momentum, and second-order momentum during the full fine-tuning process of AdamW. The results on the STSB dataset are shown in Figure 1, and additional experimental results can be found in Appendix C.1.



Table 4: GLUE benchmark results of memory-efficient fine-tuning methods using pre-trained RoBERTa-Base. We set rank as 8 for all three memory-efficient methods. We used AdamW as the optimizer in full finetuning and LoRA. MLorc and Galore refer to MLorc-AdamW and Galore-AdamW respectively. Best performances among MLorc, Lora and GaLore are highlighted in bold.

Method	CoLA	MRPC	RTE	STSB	SST2	QNLI	MNLI	QQP	AVG
Full	62.33	89.46	75.81	90.50	95.18	92.92	87.62	91.67	85.69
MLorc	<b>62.07</b>	<b>89.46</b>	<b>77.98</b>	90.59	<b>95.18</b>	<b>93.19</b>	<b>87.53</b>	90.45	<b>85.81</b>
LoRA	61.53	<b>89.46</b>	76.53	<b>90.74</b>	94.72	92.75	87.51	<b>90.91</b>	85.52
GaLore	60.34	88.24	71.12	90.50	94.38	92.42	86.84	89.76	84.20

## 5 Conclusions and future work

In this work, we introduce MLorc (Momentum Low-rank Compression), a novel memory-efficient optimization paradigm designed to bridge the gap between parameter-efficient fine-tuning and full-parameter training for large language models (LLMs). Unlike existing low-rank adaptation methods such as LoRA [Hu et al., 2022] and GaLore [Zhao et al., 2024], MLorc leverages a previously underexplored insight: momentum is low-rank, and it can be compressed without significantly breaking training dynamics. By applying Randomized SVD (RSVD) [Halko et al., 2011] to compress and reconstruct momentum states instead of gradients, MLorc achieves a better balance between memory savings and training dynamics preservation.

Through comprehensive empirical evaluations across various model architectures, optimizers (e.g., AdamW and Lion), and NLP tasks (including NLG and NLU benchmarks), we demonstrate that MLorc: (1) consistently outperforms LoRA and GaLore in terms of validation accuracy; (2) matches or exceeds full fine-tuning performance with a small compression rank (e.g.,  $r = 4$ ); (3) maintains comparable memory consumption to LoRA and achieves better time efficiency than GaLore; (4) shows strong training dynamics alignment with full fine-tuning, as evidenced by its training loss curves and optimal learning rates.

MLorc contributes to reducing the environmental impact of large-scale model training by significantly lowering GPU memory usage and computation overhead, which can lead to reduced energy consumption during fine-tuning.

Looking ahead, we identify several promising directions for future work to validate and enhance MLorc: (1) Although our experiments focus on fine-tuning, extending MLorc to large-scale pre-training holds strong potential, as demonstrated by GaLore [Zhao et al., 2024], which shows that memory-efficient training schemes can significantly reduce memory usage while preserving model quality; (2) the current approach to compress momentum may not be optimal, so exploring alternative compression strategies with improved memory/time efficiency and approximation accuracy could be valuable; (3) our experiments were limited to models up to 7B parameters, so further empirical evaluation on larger-scale models (e.g., GPT-3 [Brown et al., 2020]) would help assess the scalability and effectiveness of MLorc.

## References

- Yossi Arjevani, Yair Carmon, John C Duchi, Dylan J Foster, Nathan Srebro, and Blake Woodworth. Lower bounds for non-convex stochastic optimization. *Mathematical Programming*, 199(1):165–214, 2023.
- Dan Biderman, Jose Javier Gonzalez Ortiz, Jacob Portes, Mansheej Paul, Philip Greengard, Connor Jennings, Daniel King, Sam Havens, Vitaliy Chiley, Jonathan Frankle, et al. Lora learns less and forgets less. *CoRR*, 2024.
- Tom Brown, Benjamin Mann, Nick Ryder, Melanie Subbiah, Jared D Kaplan, Prafulla Dhariwal, Arvind Neelakantan, Pranav Shyam, Girish Sastry, Amanda Askell, et al. Language models are few-shot learners. *Advances in neural information processing systems*, 33:1877–1901, 2020.

- Mark Chen, Jerry Tworek, Heewoo Jun, Qiming Yuan, Henrique Ponde De Oliveira Pinto, Jared Kaplan, Harri Edwards, Yuri Burda, Nicholas Joseph, Greg Brockman, et al. Evaluating large language models trained on code. *arXiv preprint arXiv:2107.03374*, 2021.
- Tianqi Chen, Bing Xu, Chiyuan Zhang, and Carlos Guestrin. Training deep nets with sublinear memory cost. *arXiv preprint arXiv:1604.06174*, 2016.
- Xiangning Chen, Chen Liang, Da Huang, Esteban Real, Kaiyuan Wang, Hieu Pham, Xuanyi Dong, Thang Luong, Cho-Jui Hsieh, Yifeng Lu, et al. Symbolic discovery of optimization algorithms. *Advances in neural information processing systems*, 36:49205–49233, 2023.
- Karl Cobbe, Vineet Kosaraju, Mohammad Bavarian, Mark Chen, Heewoo Jun, Lukasz Kaiser, Matthias Plappert, Jerry Tworek, Jacob Hilton, Reiichiro Nakano, et al. Training verifiers to solve math word problems. *arXiv preprint arXiv:2110.14168*, 2021.
- Romain Cosson, Ali Jadbabaie, Anuran Makur, Amirhossein Reisizadeh, and Devavrat Shah. Low-rank gradient descent. *IEEE Open Journal of Control Systems*, 2:380–395, 2023.
- Tim Dettmers, Mike Lewis, Sam Shleifer, and Luke Zettlemoyer. 8-bit optimizers via block-wise quantization. In *International Conference on Learning Representations*, 2022.
- Tim Dettmers, Artidoro Pagnoni, Ari Holtzman, and Luke Zettlemoyer. Qlora: Efficient finetuning of quantized llms. *Advances in neural information processing systems*, 36:10088–10115, 2023.
- Yiming Dong, Huan Li, and Zhouchen Lin. Convergence rate analysis of lion. *arXiv preprint arXiv:2411.07724*, 2024.
- Nathan Halko, Per-Gunnar Martinsson, and Joel A Tropp. Finding structure with randomness: Probabilistic algorithms for constructing approximate matrix decompositions. *SIAM review*, 53(2):217–288, 2011.
- Yongchang Hao, Yanshuai Cao, and Lili Mou. Flora: Low-rank adapters are secretly gradient compressors. In *International Conference on Machine Learning*, pages 17554–17571. PMLR, 2024.
- Soufiane Hayou, Nikhil Ghosh, and Bin Yu. Lora+: Efficient low rank adaptation of large models. In *International Conference on Machine Learning*, pages 17783–17806. PMLR, 2024.
- Edward J Hu, Yelong Shen, Phillip Wallis, Zeyuan Allen-Zhu, Yuanzhi Li, Shean Wang, Lu Wang, Weizhu Chen, et al. Lora: Low-rank adaptation of large language models. *ICLR*, 1(2):3, 2022.
- Damjan Kalajdzievski. A rank stabilization scaling factor for fine-tuning with lora. *arXiv preprint arXiv:2312.03732*, 2023.
- Bingrui Li, Jianfei Chen, and Jun Zhu. Memory efficient optimizers with 4-bit states. *Advances in Neural Information Processing Systems*, 36:15136–15171, 2023.
- Dengchun Li, Yingzi Ma, Naizheng Wang, Zhengmao Ye, Zhiyuan Cheng, Yinghao Tang, Yan Zhang, Lei Duan, Jie Zuo, Cal Yang, et al. Mixlora: Enhancing large language models fine-tuning with lora-based mixture of experts. *arXiv preprint arXiv:2404.15159*, 2024.
- Xiang Lisa Li and Percy Liang. Prefix-tuning: Optimizing continuous prompts for generation. In *Proceedings of the 59th Annual Meeting of the Association for Computational Linguistics and the 11th International Joint Conference on Natural Language Processing (Volume 1: Long Papers)*, pages 4582–4597, 2021.
- Shih-Yang Liu, Maksim Khadkevich, Nai Chit Fung, Charbel Sakr, Chao-Han Huck Yang, Chien-Yi Wang, Saurav Muralidharan, Hongxu Yin, Kwang-Ting Cheng, Jan Kautz, et al. Eora: Training-free compensation for compressed llm with eigenspace low-rank approximation. *arXiv preprint arXiv:2410.21271*, 2024a.
- Shih-Yang Liu, Chien-Yi Wang, Hongxu Yin, Pavlo Molchanov, Yu-Chiang Frank Wang, Kwang-Ting Cheng, and Min-Hung Chen. Dora: Weight-decomposed low-rank adaptation. In *International Conference on Machine Learning*, pages 32100–32121. PMLR, 2024b.

- Yinhan Liu, Myle Ott, Naman Goyal, Jingfei Du, Mandar Joshi, Danqi Chen, Omer Levy, Mike Lewis, Luke Zettlemoyer, and Veselin Stoyanov. Roberta: A robustly optimized bert pretraining approach. *arXiv preprint arXiv:1907.11692*, 2019.
- Qijun Luo, Hengxu Yu, and Xiao Li. Badam: A memory efficient full parameter optimization method for large language models. *Advances in Neural Information Processing Systems*, 37:24926–24958, 2024.
- Kai Lv, Hang Yan, Qipeng Guo, Haijun Lv, and Xipeng Qiu. Adalomo: Low-memory optimization with adaptive learning rate. *CoRR*, 2023.
- Sadhika Malladi, Tianyu Gao, Eshaan Nichani, Alex Damian, Jason D Lee, Danqi Chen, and Sanjeev Arora. Fine-tuning language models with just forward passes. *Advances in Neural Information Processing Systems*, 36:53038–53075, 2023.
- Fanxu Meng, Zhaohui Wang, and Muhan Zhang. Pissa: Principal singular values and singular vectors adaptation of large language models. *Advances in Neural Information Processing Systems*, 37:121038–121072, 2024.
- Colin Raffel, Noam Shazeer, Adam Roberts, Katherine Lee, Sharan Narang, Michael Matena, Yanqi Zhou, Wei Li, and Peter J Liu. Exploring the limits of transfer learning with a unified text-to-text transformer. *Journal of machine learning research*, 21(140):1–67, 2020.
- Sahar Rajabi, Nayeema Nonta, and Sirisha Rambhatla. Subtract your grad: Gradient subspace tracking for memory and time efficient full-parameter llm training. *arXiv preprint arXiv:2502.01586*, 2025.
- Sashank J Reddi, Satyen Kale, and Sanjiv Kumar. On the convergence of adam and beyond. *arXiv preprint arXiv:1904.09237*, 2019.
- Hugo Touvron, Louis Martin, Kevin Stone, Peter Albert, Amjad Almahairi, Yasmine Babaei, Nikolay Bashlykov, Soumya Batra, Prajjwal Bhargava, Shruti Bhosale, et al. Llama 2: Open foundation and fine-tuned chat models. *arXiv preprint arXiv:2307.09288*, 2023.
- Alex Wang, Amanpreet Singh, Julian Michael, Felix Hill, Omer Levy, and Samuel Bowman. Glue: A multi-task benchmark and analysis platform for natural language understanding. In *Proceedings of the 2018 EMNLP Workshop BlackboxNLP: Analyzing and Interpreting Neural Networks for NLP*, pages 353–355, 2018.
- Bohan Wang, Huishuai Zhang, Zhiming Ma, and Wei Chen. Convergence of adagrad for non-convex objectives: Simple proofs and relaxed assumptions. In *The Thirty Sixth Annual Conference on Learning Theory*, pages 161–190. PMLR, 2023a.
- Qinsi Wang, Jinghan Ke, Masayoshi Tomizuka, Yiran Chen, Kurt Keutzer, and Chenfeng Xu. Dobi-svd: Differentiable svd for llm compression and some new perspectives. *arXiv preprint arXiv:2502.02723*, 2025.
- Yiming Wang, Yu Lin, Xiaodong Zeng, and Guannan Zhang. Multilora: Democratizing lora for better multi-task learning. *arXiv preprint arXiv:2311.11501*, 2023b.
- Wenhan Xia, Chengwei Qin, and Elad Hazan. Chain of lora: Efficient fine-tuning of language models via residual learning. In *ICML 2024 Workshop on LLMs and Cognition*, 2024.
- David H Yang, Mohammad Mohammadi Amiri, Tejaswini Pedapati, Subhajit Chaudhury, and Pin-Yu Chen. Sparse gradient compression for fine-tuning large language models. *arXiv preprint arXiv:2502.00311*, 2025.
- Longhui Yu, Weisen Jiang, Han Shi, Jincheng Yu, Zhengying Liu, Yu Zhang, James T Kwok, Zhenguo Li, Adrian Weller, and Weiyang Liu. Metamath: Bootstrap your own mathematical questions for large language models. *arXiv preprint arXiv:2309.12284*, 2023.
- Longteng Zhang, Lin Zhang, Shaohuai Shi, Xiaowen Chu, and Bo Li. Lora-fa: Memory-efficient low-rank adaptation for large language models fine-tuning. *arXiv preprint arXiv:2308.03303*, 2023a.

- Qingru Zhang, Minshuo Chen, Alexander Bukharin, Nikos Karampatziakis, Pengcheng He, Yu Cheng, Weizhu Chen, and Tuo Zhao. Adalora: Adaptive budget allocation for parameter-efficient fine-tuning. *arXiv preprint arXiv:2303.10512*, 2023b.
- Zhenyu Zhang, Ajay Jaiswal, Lu Yin, Shiwei Liu, Jiawei Zhao, Yuandong Tian, and Zhangyang Wang. Q-galore: Quantized galore with int4 projection and layer-adaptive low-rank gradients. *arXiv preprint arXiv:2407.08296*, 2024.
- Jiawei Zhao, Florian Tobias Schaefer, and Anima Anandkumar. Zero initialization: Initializing neural networks with only zeros and ones. *Transactions on Machine Learning Research*, 2022.
- Jiawei Zhao, Zhenyu Zhang, Beidi Chen, Zhangyang Wang, Anima Anandkumar, and Yuandong Tian. Galore: Memory-efficient llm training by gradient low-rank projection. In *International Conference on Machine Learning*, pages 61121–61143. PMLR, 2024.
- Tianyu Zheng, Ge Zhang, Tianhao Shen, Xueling Liu, Bill Yuchen Lin, Jie Fu, Wenhui Chen, and Xiang Yue. Opencodeinterpreter: Integrating code generation with execution and refinement. In *Findings of the Association for Computational Linguistics ACL 2024*, pages 12834–12859, 2024.
- Bojia Zi, Xianbiao Qi, Lingzhi Wang, Jianan Wang, Kam-Fai Wong, and Lei Zhang. Delta-lora: Fine-tuning high-rank parameters with the delta of low-rank matrices. *arXiv preprint arXiv:2309.02411*, 2023.

# Appendix

Appendix is organized as follows. Appendix A introduces details on RSVD. Appendix B provides a complete proof of Theorem 3.4. Appendix C presents additional experimental evidence on the low-rank structure and memory efficiency of MLorc. Appendix D gives detailed hyperparameter settings of experiments in Section 4 for reproducibility.

## A Details on RSVD

Randomized Singular Value Decomposition (RSVD) is an efficient algorithm for computing a low-rank approximation of large matrices. Unlike the classical SVD, which can be computationally expensive for large-scale data, RSVD uses random projections to reduce the dimensionality of the input matrix before performing decomposition. This significantly accelerates the computation while retaining high approximation accuracy.

---

### Algorithm 3 Randomized SVD (RSVD) with Oversampling

---

**Require:** Matrix  $A \in \mathbb{R}^{m \times n}$ , target rank  $r$ , oversampling parameter  $p$

**Ensure:** Approximate rank- $r$  SVD:  $A \approx U \Sigma V^\top$

$l \leftarrow r + p$

Generate a random Gaussian matrix  $\Omega \in \mathbb{R}^{n \times l}$

$Y \leftarrow A\Omega \in \mathbb{R}^{m \times l}$

Compute the QR decomposition:  $Y = QR$

$B \leftarrow Q^\top A \in \mathbb{R}^{l \times n}$

Compute SVD of the small matrix:  $\tilde{U}, \Sigma, V^\top = \text{SVD}(B)$

$U \leftarrow Q\tilde{U}$

**return**  $U, \Sigma, V$

---

The key idea behind RSVD is to first project the original matrix  $A \in \mathbb{R}^{m \times n}$  onto a lower-dimensional subspace using a random matrix  $\Omega$  producing a smaller matrix  $Y = A\Omega$ . Then, it performs a standard SVD or QR decomposition on  $Y$ , and reconstructs the approximate SVD  $A$  from this compressed representation.

Concerning the precision of RSVD, we have the following theorem, which is Theorem 10.5 of [Halko et al., 2011]:

**Lemma A.1** (Approximation error bound of RSVD). *Let  $A \in \mathbb{R}^{m \times n}$  have singular values  $\sigma_1 \geq \sigma_2 \geq \dots$ . For a target rank  $r$  and oversampling parameter  $p$ , define  $l = r + p$ . Then, the randomized SVD algorithm produces an approximation  $A_{RS}$  such that*

$$\mathbb{E} [\|A - A_{RS}\|_F] \leq \left(1 + \frac{r}{p-1}\right)^{\frac{1}{2}} \left(\sum_{j>r} \sigma_j^2\right)^{\frac{1}{2}}. \quad (2)$$

This lemma suggests that when the desired rank  $r$  is small (e.g.,  $r = 4$ ), with a proper oversampling parameter  $p$ , RSVD has the same level approximation error (in expectation) as exact SVD up to a constant. We note that though the oversampling parameter  $p$  is involved in providing an error bound for RSVD, empirically, it does not significantly influence the experimental result. To reduce computational overhead, we set oversampling parameter  $p = 0$  in each of our experiments.

## B Proofs

Our proof generally follows that of [Dong et al., 2024], while additionally analyzing and bounding the error introduced by the low-rank compression in MLorc.

## B.1 Lemmas

**Lemma B.1.** *Under Assumption 3.3, we have*

$$\|\tilde{m}^k - m_t\|_F \leq \gamma_1 \|c_t\|_F + \gamma_2 \|g_t\|_F$$

where  $\gamma_1 = \rho \frac{\beta_2}{\beta_1} \left(1 + \frac{r}{p-1}\right)^{\frac{1}{2}}$ ,  $\gamma_2 = \rho \left| (1 - \beta_2) - \frac{\beta_2(1-\beta_1)}{\beta_1} \right| \left(1 + \frac{r}{p-1}\right)^{\frac{1}{2}}$ .

*Proof.* Suppose  $\sigma_1^t \geq \sigma_2^t \geq \dots$  are  $m_t$ 's singular values. According to Assumption 3.3, we have

$$\begin{aligned} \left( \sum_{j>r} (\sigma_j^t)^2 \right)^{\frac{1}{2}} &\leq \rho \|m_t\|_F = \rho \left\| \frac{\beta_2}{\beta_1} c_t + \left[ (1 - \beta_2) - \frac{\beta_2(1 - \beta_1)}{\beta_1} \right] g_t \right\|_F \\ &\leq \rho \frac{\beta_2}{\beta_1} \|c_t\|_F + \rho \left| (1 - \beta_2) - \frac{\beta_2(1 - \beta_1)}{\beta_1} \right| \|g_t\|_F. \end{aligned}$$

According to Lemma A.1, we have

$$\|\tilde{m}^k - m_t\|_F \leq \left(1 + \frac{r}{p-1}\right)^{\frac{1}{2}} \left( \sum_{j>r} (\sigma_j^t)^2 \right)^{\frac{1}{2}} \leq \gamma_1 \|c_t\|_F + \gamma_2 \|g_t\|_F$$

where  $\gamma_1 = \rho \frac{\beta_2}{\beta_1} \left(1 + \frac{r}{p-1}\right)^{\frac{1}{2}}$ ,  $\gamma_2 = \rho \left| (1 - \beta_2) - \frac{\beta_2(1-\beta_1)}{\beta_1} \right| \left(1 + \frac{r}{p-1}\right)^{\frac{1}{2}}$ . □

**Lemma B.2.** *Denote  $\delta_t = c_t - \nabla f(W_t)$ . Under Assumption 3.1, 3.2 and 3.3, we have*

$$\begin{aligned} \frac{1}{T} \sum_{k=1}^T \mathbb{E} [\|\delta_t\|_{1,1}] &\leq \frac{\sqrt{d}\sigma}{\sqrt{b}T(1-\beta_2)} + \frac{2L\alpha d}{1-\beta_2} + (|\beta_1 - \beta_2| + (1 - \beta_1)) \cdot \frac{\sqrt{d}\sigma}{\sqrt{b}(1-\beta_2)} \\ &\quad + \frac{1}{T} \sum_{t=1}^{T-1} \frac{\beta_1 \sqrt{d} \gamma_2}{1-\beta_2} \mathbb{E} [\|\nabla f(W_t)\|_{1,1}] + \frac{\beta_1 \sqrt{d} \gamma_2}{1-\beta_2} \frac{\sigma}{\sqrt{b}} \\ &\quad + \frac{1}{T} \sum_{t=1}^{T-1} \frac{\beta_1 \sqrt{d} \gamma_1}{1-\beta_2} \mathbb{E} [\|c_t\|_{1,1}]. \end{aligned}$$

*Proof.* Denote  $\xi_t = g_t - \nabla f(W_t)$ . We have

$$\begin{aligned} \delta_t &= \beta_1 \tilde{m}_{t-1} + (1 - \beta_1) g_t - \nabla f(W_t) \\ &= \beta_1 (\tilde{m}_{t-1} - m_{t-1}) + \beta_1 \beta_2 \tilde{m}_{t-2} + \beta_1 (1 - \beta_2) \nabla f(W_{t-1}) + (1 - \beta_1) g_t - \nabla f(W_t) \\ &= \beta_1 (\tilde{m}_{t-1} - m_{t-1}) + \beta_2 (c_{t-1} - (1 - \beta_1) \nabla f(W_{t-1})) + \beta_1 (1 - \beta_2) \nabla f(W_{t-1}) + (1 - \beta_1) g_t - \nabla f(W_t) \\ &= \beta_1 (\tilde{m}_{t-1} - m_{t-1}) + \beta_2 (\delta_{t-1} + \nabla f(W_{t-1})) - \beta_2 (1 - \beta_1) g_{t-1} + \beta_1 (1 - \beta_2) \nabla f(W_{t-1}) + (1 - \beta_1) g_t - \nabla f(W_t) \\ &= \beta_1 (\tilde{m}_{t-1} - m_{t-1}) + \beta_2 (\delta_{t-1} + \nabla f(W_{t-1})) + (\beta_1 - \beta_2) (\xi_{t-1} + \nabla f(W_{t-1})) + (1 - \beta_1) (\xi_t + \nabla f(W_t)) - \nabla f(W_t) \\ &= \beta_1 (\tilde{m}_{t-1} - m_{t-1}) + \beta_2 \delta_{t-1} - \beta_1 (\nabla f(W_t) - \nabla f(W_{t-1})) + (\beta_1 - \beta_2) \xi_{t-1} + (1 - \beta_1) \xi_t \\ &= \beta_2^{t-1} \delta_1 + \sum_{k=2}^t \beta_2^{t-k} \left( -\beta_1 (\nabla f(W_k) - \nabla f(W_{k-1})) + (\beta_1 - \beta_2) \xi_{k-1} + (1 - \beta_1) \xi_k + \beta_1 (\tilde{m}_{k-1} - m_{k-1}) \right) \\ &= \beta_2^{t-1} \delta_1 - \beta_1 \sum_{k=2}^t \beta_2^{t-k} (\nabla f(W_k) - \nabla f(W_{k-1})) + (\beta_1 - \beta_2) \sum_{k=2}^t \beta_2^{t-k} \xi_{k-1} \\ &\quad + (1 - \beta_1) \sum_{k=2}^t \beta_2^{t-k} \xi_k + \beta_1 \sum_{k=2}^t \beta_2^{t-k} (\tilde{m}_{k-1} - m_{k-1}). \end{aligned}$$



Taking expectations, and according to Lemma B.2, we have

$$\begin{aligned}
\mathbb{E} [\|\delta_t\|_{1,1}] &\leq \sqrt{d} \left\{ \underbrace{\beta_2^{t-1} \mathbb{E} [\|\delta_1\|_F] + \beta_1 \sum_{k=2}^t \beta_2^{t-k} \mathbb{E} [\|\nabla f(W_k) - \nabla f(W_{k-1})\|_F]}_{\text{term (a)}} \right. \\
&\quad + \underbrace{\mathbb{E} \left[ \left\| (\beta_1 - \beta_2) \sum_{k=2}^t \beta_2^{t-k} \xi_{k-1} + (1 - \beta_1) \sum_{k=2}^t \beta_2^{t-k} \xi_k \right\|_F \right]}_{\text{term (b)}} \\
&\quad \left. + \underbrace{\beta_1 \sum_{k=2}^t \beta_2^{t-k} \mathbb{E} [\|\tilde{m}_{k-1} - m_{k-1}\|_F]}_{\text{term (c)}} \right\}.
\end{aligned}$$

For term (a), we have

$$\begin{aligned}
\text{term (a)} &\leq L \sum_{k=2}^t \beta_2^{t-k} \mathbb{E} [\|W_k - W_{k-1}\|_F] \\
&= L\alpha \sum_{k=2}^t \beta_2^{t-k} \mathbb{E} [\|\text{sign}(c^{t-1})\|_F] \\
&\leq 2L\alpha\sqrt{d} \sum_{k=2}^t \beta_2^{t-k} \\
&\leq \frac{2L\alpha\sqrt{d}}{1 - \beta_2}.
\end{aligned}$$

For term (b), we have

$$\begin{aligned}
\text{term (b)} &\leq |\beta_1 - \beta_2| \mathbb{E} \left[ \left\| \sum_{k=2}^t \beta_2^{t-k} \xi_{k-1} \right\|_F \right] + (1 - \beta_1) \mathbb{E} \left[ \left\| \sum_{k=2}^t \beta_2^{t-k} \xi_k \right\|_F \right] \\
&\leq |\beta_1 - \beta_2| \sqrt{\mathbb{E} \left[ \left\| \sum_{k=2}^t \beta_2^{t-k} \xi_{k-1} \right\|_F^2 \right]} + (1 - \beta_1) \sqrt{\mathbb{E} \left[ \left\| \sum_{k=2}^t \beta_2^{t-k} \xi_k \right\|_F^2 \right]} \\
&= |\beta_1 - \beta_2| \sqrt{\sum_{k=2}^t \beta_2^{2(t-k)} \mathbb{E} [\|\xi_{k-1}\|_F^2]} + (1 - \beta_1) \sqrt{\sum_{k=2}^t \beta_2^{2(t-k)} \mathbb{E} [\|\xi_k\|_F^2]} \\
&= |\beta_1 - \beta_2| \sqrt{\sigma^2 \sum_{k=2}^t \beta_2^{2(t-k)} / b} + (1 - \beta_1) \sqrt{\sigma^2 \sum_{k=2}^t \beta_2^{2(t-k)} / b} \\
&\leq (|\beta_1 - \beta_2| + (1 - \beta_1)) \cdot \frac{\sigma}{\sqrt{b(1 - \beta_2^2)}} \\
&\leq (|\beta_1 - \beta_2| + (1 - \beta_1)) \cdot \frac{\sigma}{\sqrt{b(1 - \beta_2)}}.
\end{aligned}$$

For term (c), according to Lemma B.1, we have

$$\begin{aligned}
\text{term (c)} &\leq \sum_{k=2}^t \beta_2^{t-k} \mathbb{E} [\|\tilde{m}_{k-1} - m_{k-1}\|_F] \\
&\leq \gamma_1 \sum_{k=2}^t \beta_2^{t-k} \mathbb{E} [\|c_{k-1}\|_F] + \gamma_2 \sum_{k=2}^t \beta_2^{t-k} \mathbb{E} [\|g_{k-1}\|_F] \\
&\leq \gamma_1 \sum_{k=2}^t \beta_2^{t-k} \mathbb{E} [\|c_{k-1}\|_F] + \gamma_2 \sum_{k=2}^t \beta_2^{t-k} \mathbb{E} [\|\nabla f(W_{k-1})\|_F] + \gamma_2 \sum_{k=2}^t \beta_2^{t-k} \mathbb{E} [\|\xi_{k-1}\|_F] \\
&\leq \gamma_1 \sum_{k=2}^t \beta_2^{t-k} \mathbb{E} [\|c_{k-1}\|_{1,1}] + \gamma_2 \sum_{k=2}^t \beta_2^{t-k} \mathbb{E} [\|\nabla f(W_{k-1})\|_{1,1}] + \sigma \gamma_2 / (\sqrt{b}(1 - \beta_2)).
\end{aligned}$$

Plugging terms (a), (b), (c) back, we get

$$\begin{aligned}
\mathbb{E} [\|\delta_t\|_{1,1}] &\leq \sqrt{d} \{ \beta_2^{k-1} \mathbb{E} [\|\delta_1\|_F] + \frac{2\beta_1 L \alpha \sqrt{d}}{1 - \beta_2} + (|\beta_1 - \beta_2| + (1 - \beta_1)) \cdot \frac{\sigma}{\sqrt{b(1 - \beta_2)}} \} \\
&\quad + \sqrt{d} \gamma_2 \beta_1 \sum_{k=2}^t \beta_2^{t-k} \mathbb{E} [\|\nabla f(W_{k-1})\|_{1,1} / (1 - \beta_2)] + \beta_1 \sigma \sqrt{d} \gamma_2 / (\sqrt{b}(1 - \beta_2)) \\
&\quad + \sqrt{d} \beta_1 \gamma_1 \sum_{k=2}^t \beta_2^{t-k} \mathbb{E} [\|c_{k-1}\|_{1,1} / (1 - \beta_2)].
\end{aligned}$$

Initializing  $m_0 = g_1$ , we have  $\mathbb{E} [\|\delta_1\|_F] = \mathbb{E} [\|g_1 - \nabla f(W_1)\|_F] \leq \sigma / \sqrt{b}$ , and

$$\begin{aligned}
\frac{1}{T} \sum_{t=1}^T \mathbb{E} [\|\delta_t\|_{1,1}] &\leq \frac{\sqrt{d} \sigma}{\sqrt{b} T (1 - \beta_2)} + \frac{2L \alpha d}{1 - \beta_2} + (|\beta_1 - \beta_2| + (1 - \beta_1)) \cdot \frac{\sqrt{d} \sigma}{\sqrt{b(1 - \beta_2)}} \\
&\quad + \frac{1}{T} \sum_{t=1}^{T-1} \frac{\beta_1 \sqrt{d} \gamma_2}{1 - \beta_2} \mathbb{E} [\|\nabla f(W_t)\|_{1,1}] + \frac{\beta_1 \sqrt{d} \gamma_2}{1 - \beta_2} \frac{\sigma}{\sqrt{b}} \\
&\quad + \frac{1}{T} \sum_{t=1}^{T-1} \frac{\beta_1 \sqrt{d} \gamma_1}{1 - \beta_2} \mathbb{E} [\|c_t\|_{1,1}].
\end{aligned}$$

□

## B.2 Proof of Theorem 3.4

**Formal statement of Theorem 3.4:** Suppose Assumptions 3.1, 3.2 and 3.3 hold. Denote  $\kappa = \left| 1 - \frac{\beta_2(1-\beta_1)}{\beta_1(1-\beta_2)} \right|$ . If  $\kappa \neq 0$ , we assume

$$\rho \leq \min \left\{ \frac{1 - \beta_2}{8\beta_2 \sqrt{d(1 + r/(p-1))}}, \frac{1 - \beta_2}{8\kappa \sqrt{d(1 + r/(p-1))}} \right\}.$$

If  $\kappa = 0$ , we assume

$$\rho \leq \frac{1 - \beta_2}{8\beta_2 \sqrt{d(1 + r/(p-1))}}.$$

Then, we have

$$\begin{aligned}
\frac{1}{T} \sum_{t=1}^T \mathbb{E} [\|\nabla f(W_t)\|_{1,1} + \|c_t\|_{1,1}] &\leq O(1) \left[ \frac{f(W_1) - f(W_T)}{\alpha T} + \frac{\sigma \sqrt{d}}{\sqrt{b} T (1 - \beta_2)} \right. \\
&\quad \left. + \frac{2L \alpha \beta_1 d}{1 - \beta_2} + dL \alpha + \frac{(1 - \beta_2) \sigma \sqrt{d}}{\sqrt{b}} + (|\beta_1 - \beta_2| + 1 - \beta_1) \cdot \frac{\sqrt{d} \sigma}{\sqrt{b(1 - \beta_2)}} \right],
\end{aligned}$$

Denote  $f(W_1) - \inf_W f(W) = \Delta$ . We can set  $b = O(1)$ ,  $1 - \beta_1 = \Theta(d^{-1}\sigma^{-2}\epsilon^2)$ ,  $1 - \beta_2 = \Theta(d^{-1}\sigma^{-2}\epsilon^2)$ ,  $\alpha = \Theta(d^{-2}L^{-1}\sigma^{-2}\epsilon^3)$ ,  $T = \Theta(\Delta L\sigma^2 d^2 \epsilon^{-4})$ , and get

$$\frac{1}{T} \sum_{t=1}^T \mathbb{E} [\|\nabla f(W_t)\|_{1,1}] \leq O(\epsilon).$$

Thus, we can find  $t = O(\Delta L d^2 \sigma^2 \epsilon^{-4})$  such that  $\mathbb{E}[\|\nabla f(W_t)\|_{1,1}] \leq O(\epsilon)$ .

*Proof.* According to Assumption 3.1, we have

$$\begin{aligned} & f(W_{t+1}) - f(W_t) \\ & \leq \langle \nabla f(W_t), W_{t+1} - W_t \rangle + \frac{L}{2} \|W_{t+1} - W_t\|_F^2 \\ & = -\alpha \langle \nabla f(W_t), \text{sign}(c_t) \rangle + \frac{L\alpha^2}{2} \|\text{sign}(c_t)\|_F^2 \\ & = -\alpha \langle \nabla f(W_t), \text{sign}(c_t) \rangle / 2 - \alpha \langle \nabla f(W_t), \text{sign}(c_t) \rangle / 2 + \frac{L\alpha^2}{2} \|\text{sign}(c_t)\|_F^2 \\ & = -\alpha \langle \nabla f(W_t), \text{sign}(\nabla f(W_t)) \rangle / 2 - \alpha \langle \nabla f(W_t), \text{sign}(c_t) - \text{sign}(\nabla f(W_t)) \rangle / 2 \\ & \quad - \alpha \langle c_t, \text{sign}(c_t) \rangle / 2 - \alpha \langle \nabla f(W_t) - c_t, \text{sign}(c_t) \rangle / 2 + \frac{L\alpha^2}{2} \|\text{sign}(c_t)\|_F^2 \\ & \leq -\alpha \|\nabla f(W_t)\|_{1,1} / 2 - \alpha \|c_t\|_{1,1} / 2 + 2\alpha \|\delta_t\|_{1,1} + \frac{dL\alpha^2}{2} \end{aligned}$$

Taking expectations, and according to Lemma B.2, we have

$$\begin{aligned} & \mathbb{E}[f(W_{t+1})] - f(W_1) \\ & \leq -\alpha \sum_{t=1}^T \mathbb{E}[\|\nabla f(W_t)\|_{1,1} + \|c_t\|_{1,1}] / 2 + 2\alpha \sum_{k=1}^T \mathbb{E}[\|\delta_k\|_{1,1}] + TdL\alpha^2 / 2 \\ & \leq -\alpha \sum_{t=1}^T \mathbb{E}[\|\nabla f(W_t)\|_{1,1} + \|c_t\|_{1,1}] / 2 \\ & \quad + 2\alpha T \left\{ \frac{\sqrt{d}\sigma}{\sqrt{b}T(1-\beta_2)} + \frac{2L\alpha\beta_1 d}{1-\beta_2} + (|\beta_1 - \beta_2| + 1 - \beta_1) \cdot \frac{\sqrt{d}\sigma}{\sqrt{b}(1-\beta_2)} \right. \\ & \quad \left. + \frac{1}{T} \sum_{t=1}^{T-1} \frac{\beta_1 \sqrt{d}\gamma_2}{1-\beta_2} \mathbb{E}[\|\nabla f(W_t)\|_{1,1}] + \frac{\beta_1 \sqrt{d}\gamma_2}{1-\beta_2} \frac{\sigma}{\sqrt{b}} + \frac{1}{T} \sum_{t=1}^{T-1} \frac{\beta_1 \sqrt{d}\gamma_1}{1-\beta_2} \mathbb{E}[\|c_t\|_{1,1}] \right\} + TdL\alpha^2 / 2. \end{aligned}$$

Denote  $\kappa = \left| 1 - \frac{\beta_2(1-\beta_1)}{\beta_1(1-\beta_2)} \right|$ . If  $\kappa \neq 0$ , we assume

$$\rho \leq \min \left\{ \frac{1-\beta_2}{8\beta_2\sqrt{d(1+r/(p-1))}}, \frac{1-\beta_2}{8\kappa\sqrt{d(1+r/(p-1))}} \right\}.$$

If  $\kappa = 0$ , we assume

$$\rho \leq \frac{1-\beta_2}{8\beta_2\sqrt{d(1+r/(p-1))}}.$$

Then, we have

$$\begin{aligned} \frac{\beta_1 \sqrt{d}\gamma_1}{1-\beta_2} &= \frac{\rho\beta_2\sqrt{d}\left(1+\frac{r}{p-1}\right)^{\frac{1}{2}}}{1-\beta_2} \leq \frac{1}{8} \\ \frac{\beta_1 \sqrt{d}\gamma_2}{1-\beta_2} &= \rho\kappa\sqrt{d}\left(1+\frac{r}{p-1}\right)^{\frac{1}{2}} \leq \frac{1-\beta_2}{8} \end{aligned}$$

And, we have

$$\begin{aligned} \frac{1}{T} \sum_{t=1}^T \mathbb{E} \left[ \|\nabla f(W_t)\|_{1,1} + \|c_t\|_{1,1} \right] &\leq O(1) \left[ \frac{f(W_1) - f(W_T)}{\alpha T} + \frac{\sigma\sqrt{d}}{\sqrt{b}T(1-\beta_2)} \right. \\ &\quad \left. + \frac{2L\alpha\beta_1 d}{1-\beta_2} + dL\alpha + \frac{(1-\beta_2)\sigma\sqrt{d}}{\sqrt{b}} + (|\beta_1 - \beta_2| + 1 - \beta_1) \cdot \frac{\sqrt{d}\sigma}{\sqrt{b(1-\beta_2)}} \right], \end{aligned}$$

Denote  $f(W_1) - \inf_W f(W) = \Delta$ . We can set  $b = O(1)$ ,  $1 - \beta_1 = \Theta(d^{-1}\sigma^{-2}\epsilon^2)$ ,  $1 - \beta_2 = \Theta(d^{-1}\sigma^{-2}\epsilon^2)$ ,  $\alpha = \Theta(d^{-2}L^{-1}\sigma^{-2}\epsilon^3)$ ,  $T = \Theta(\Delta L\sigma^2 d^2 \epsilon^{-4})$ , and get

$$\frac{1}{T} \sum_{t=1}^T \mathbb{E} \left[ \|\nabla f(W_t)\|_{1,1} \right] \leq O(\epsilon).$$

Thus, we can find  $t = O(\Delta L d^2 \sigma^2 \epsilon^{-4})$  such that  $\mathbb{E}[\|\nabla f(W_t)\|_{1,1}] \leq O(\epsilon)$ . □

## C Additional Experimental Results

### C.1 Low-rank Structures of the Gradients and Momenta

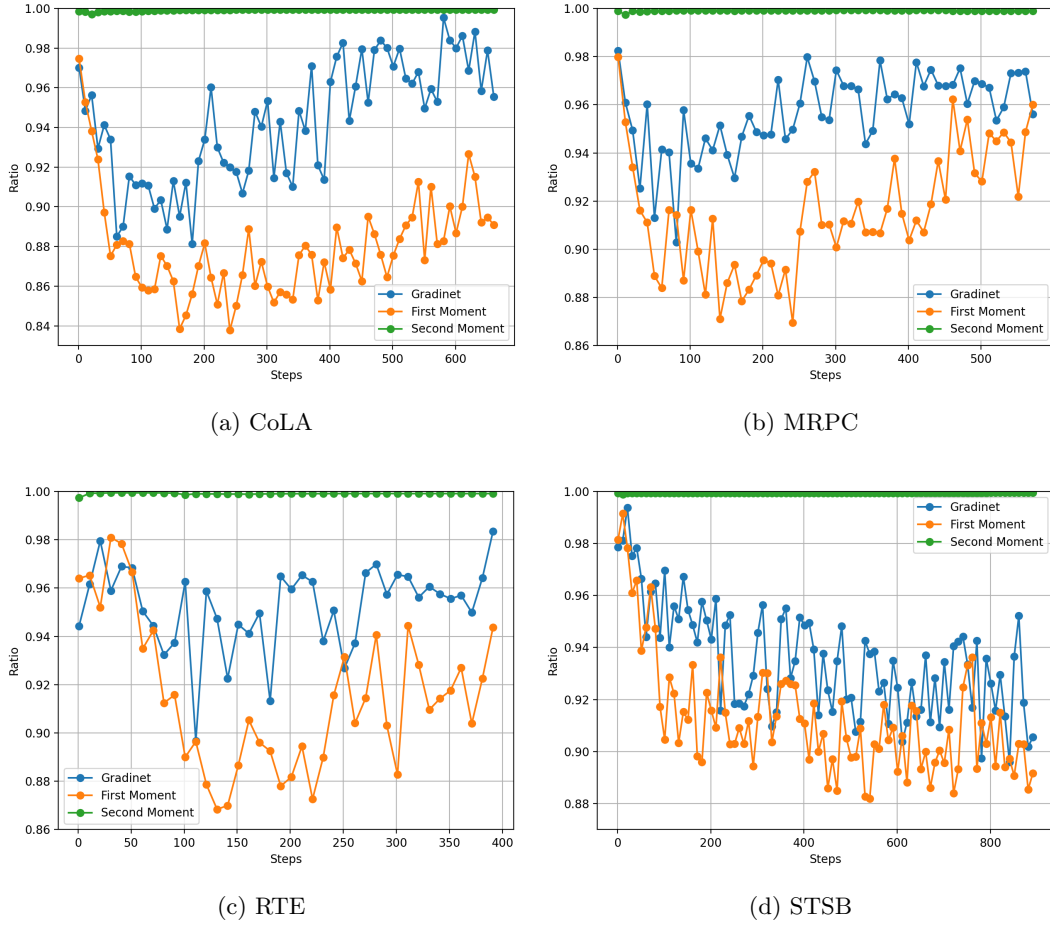


Figure 4: Ratio of top-8 singular values to total singular values for gradient, first moment, and second moment during AdamW finetuning of RoBERTa-base on the CoLA, MRPC, RTE, STSB datasets.

We conduct experiments examining the concentration of singular values in gradients and momenta during AdamW finetuning of RoBERTa-base on the CoLA, MRPC, RTE and STSB datasets. We

set the batch size as 128, epochs as 20, learning rate as 1e-4 for all these four datasets. We use AdamW finetune the matrix parameters of query, key, value, output weights in attention layers and the intermediate and output weights in feed-forward layers. We conducted these experiments on NVIDIA RTX 6000 Ada GPUs. The average ratios of top-8 singular values to total singular values for gradient, first moment, and second moment of all these matrix parameters are reported in Figure 4. We can note that, in general, the momenta on all these datasets have highly concentrated singular values and exhibit low-rank structures, which is aligned with the intuition of our method.

## C.2 Memory Footprint with Per-layer Weight Updates

As mentioned in Section 3.2, we can avoid storing full gradients in MLorc by using per-layer weight updates. Here we compare the memory consumption of LoRA and MLorc with per-layer weight updates with a batch size of 4.

Table 5: Memory footprint of MLorc with per-layer weight updates and LoRA with a batch size of 4. Apart from batch size, other hyperparameters and settings are same as previous experiments.

MLorc(per-layer update)	LoRA(default)
16.8GB	17.7GB

Table 5 suggests that MLorc can even be more memory-efficient than LoRA with per-layer weight updates, which supports our claim in Section 3.2.

## D Detailed Experimental Settings

### D.1 Fine-Tuning on MetaMathQA and CodeFeedback

The pre-trained LLaMA2-7B model is from Hugging Face<sup>1</sup>. We have reported our batch size, epoch and other settings in Section 4.1. Also, for all methods, on GSM8K dataset, the max sequence length is 512; on CodeFeedback dataset, the max sequence length is 1024; the weight decay is 0. For GaLore, the subspace update frequency  $T$  is set to 300 on both datasets. Oversampling parameter  $p$  is set as 0 for MLorc on both datasets. The temperature for evaluation is 0.8 for math task and 0.1 for coding task, since a high temperature would lead to highly unstable performance on HumanEval dataset. For each method and each dataset, the learning rate is individually tuned. We present specific learning rates in Table 6.

Table 6: Learning rates of different methods when fine-tuning on MetaMathQA and CodeFeedback dataset.

	MLorc-AdamW	Full(AdamW)	LoRA	GaLore	MLorc-Lion	Full(Lion)
MetaMathQA	7E-05	4E-05	1E-03	3E-03	1E-05	3E-05
CodeFeedback	7E-05	9E-05	3E-04	2E-03	7E-06	2E-05

### D.2 Fine-Tuning on GLUE

The pre-trained RoBERTa-Base model is from Hugging Face<sup>2</sup>. We use the same batch size, number of epochs, and maximum sequence length across all methods, including Full fine-tuning, MLorc, LoRA, and GaLore. For each method and each dataset, the learning rate is individually tuned. The LoRA scaling factor  $\alpha$  is set to 16 for all tasks. For GaLore, the subspace update frequency  $T$  is set to 50 for CoLA, MRPC, RTE, and STSB, and 100 for SST2, QNLI, MNLI, and QQP. We set the oversampling parameter  $p$  as 0 for MLorc for all datasets. Experiments for CoLA, MRPC, and RTE are conducted on NVIDIA H100 GPUs; STSB, SST2, and QNLI are conducted on NVIDIA RTX A6000 GPUs;

<sup>1</sup><https://huggingface.co/meta-llama/Llama-2-7b-chat-hf>

<sup>2</sup>[https://huggingface.co/docs/transformers/model\\_doc/roberta](https://huggingface.co/docs/transformers/model_doc/roberta)

MNLI on NVIDIA RTX 6000 Ada GPUs; and QQP on NVIDIA GeForce RTX 3090 GPUs. Detailed hyperparameter settings are provided in Table 7.

Table 7: Hyperparameter settings for the GLUE tasks. "LR" denotes the learning rate.

	CoLA	MRPC	RTE	STSB	SST2	QNLI	MNLI	QQP
Batch Size	128	128	128	128	128	128	128	128
Epochs	10	10	10	20	10	5	5	5
Max Seq. Len.	64	256	256	128	128	256	256	256
LR of Full	3E-05	7E-05	3E-05	1E-04	7E-06	1E-05	3E-05	7E-05
LR of MLorc	3E-05	7E-05	5E-05	7E-05	5E-05	5E-05	1E-04	7E-05
LR of LoRA	1E-03	1E-03	7E-04	5E-04	3E-04	5E-04	3E-04	5E-04
LR of GaLore	3E-04	5E-04	5E-04	3E-04	3E-04	3E-04	3E-04	3E-04